Biosensors and Bioelectronics 65 (2015) 327–332

Contents lists available at ScienceDirect

Biosensors and Bioelectronics

journal homepage: www.elsevier.com/locate/bios

# Quantum dots and duplex-specific nuclease enabled ultrasensitive detection and serotyping of Dengue viruses in one step in a single tube

Wei Shen, Zhiqiang Gao *

*Department of Chemistry, National University of Singapore, Singapore 117543, Singapore*

ARTICLE INFO

*Article history:*
Received 2 September 2014
Received in revised form
21 October 2014
Accepted 27 October 2014
Available online 30 October 2014

*Keywords:*
Quantum dot
Duplex-specific nuclease
Dengue virus
Fluorescence
Biosensor.

ABSTRACT

Leveraging on the enzymatic processing of Dengue virus (DV) RNA hybridized quantum dot-capped DNA capture probes (QD–CPs), an ultrasensitive assay for the detection and serotyping of DVs is described in the report. Briefly, DV-specific DNA CPs are first capped by QDs and then conjugated to magnetic beads. In a sample solution, strands of DV RNA form heteroduplexes with the QD–CPs on the magnetic beads. The CPs together with the QDs in the heteroduplexes are subsequently cleaved off the magnetic beads by a duplex-specific nuclease (DSN), releasing the QDs to the solution, freeing the target RNA strands, and availing them for another around of hybridization with the remaining QD–CPs. After removing the magnetic beads along with unreacted (uncleaved) QD–CPs by using a permanent magnet, ultrasensitive fluorescent detection of DV is realized through the cleaved QDs. Serotyping of DV is accomplished by a judicious design of the QD–CPs. The assay combines excellent signal generation by the highly fluorescent QDs and the effortlessness of utilizing magnetic beads in the removal of the unreacted QD–CPs. The highly efficient DSN cleavage in conjunction with its excellent mismatch discrimination ability permits serotyping of DVs in one tube with excellent sensitivity and selectivity.



## 1. Introduction

Dengue virus (DV) poses significant global health risks for people living in the tropical and subtropical regions. The global prevalence of Dengue has grown dramatically in the past century with around 100 million cases of acute febrile disease each year (Scott, 2007). Although many infections are mild or asymptomatic, 5–10% of patients may experience severe and fatal Dengue hemorrhagic fever and hemorrhagic shock syndrome that claim more than 12,000 lives every year (Gubler, 1998). In spite of extensive research efforts, no vaccines for Dengue are yet available (Whitehead et al., 2007). The most effective prevention is to arrest the multiplication of mosquito vectors. On the other hand, the first clinical syndromes are not reliable means for diagnosing DV infection since similar syndromes are often observed in many other virus infections. Dengue diagnosis based on clinical syndromes must be verified by laboratory tests because more than half of infected individuals either are asymptomatic or have a mild undifferentiated fever (Endy et al., 2002). Early and rapid detection of DV infection during the febrile period is crucial for proper patient management and prevention of disease spread. Apart from vector control, the burden of Dengue on society can also be reduced through appropriate and timely clinical interventions to prevent severe morbidity and mortality. The clinical diagnosis of Dengue is mainly based on the physiological symptoms and physical examination; this is especially adopted in Dengue endemic areas (Whitehorn and Farrar, 2010). However, the symptoms of Dengue infection in the first few days are difficult to differentiate from other viral infections.

There is a great demand for the rapid detection and differentiation of DV infection in order to provide timely clinical treatment and etiologic investigation and disease control. A simple, highly sensitive and selective, and easy to use assay is needed for routine DV screening especially in the resource-limited rural healthcare settings where Dengue is endemic. Based on the nature of the target (analyte), laboratory diagnosis of DV infection can be classified to the detection of (1) specific virus, (2) viral antigen, (3) genomic sequence, and (4) antibody (World Health Organization, 1997). Considered as the “gold standard” for virus identification, the diagnosis of DV infection may be unambiguously confirmed by microbiological laboratory testing (Wiwanitkit, 2010).

With the backdrop of frequent outbreaks of Dengue all over tropical and subtropical countries, the cell microbiological laboratory tests are increasingly being replaced by viral antigen detection, specific antibodies (serology), and nucleic acid detection by PCR (Guzman et al., 2010). Among them, PCR-based nucleic acid assays and quantitative PCR (qPCR) in particular, are more sensitive than the antigen assays. Despite its excellent sensitivity and

* Corresponding author. Fax: +65 6779 1691.
*E-mail address:* chmgaoz@nus.edu.sg (Z. Gao).

http://dx.doi.org/10.1016/j.bios.2014.10.060
0956-5663/

acceptable specificity, widespread applications of qPCR at point-of-care are severely hindered by the stringent demands on sample preparation and the requirement for the complex instruments in signal readout (World Health Organization, 2014; Pritchard et al., 2012). More seriously, qPCR is subject to false-negative results and all tests may be negative in the early stage of DV infection (Gijavanekar, 2011; Ranjit and Kissoon, 2011).

The above-mentioned assays are only of diagnostic value during the acute phase of the illness. Therefore, there is an ever-increasing need for rapid and accurate diagnostic assays to detect DVs at point-of-care. In this work, we developed a simple and ultrasensitive assay for the detection and serotyping of all four DVs in one step in a single tube through engaging an isothermal target cycling amplification process. The amplification was facilitated by a duplex-specific nuclease (DSN) and the uses of quantum dots (QDs) as signal generators. Comparing to organic dyes, QDs are 20 times brighter and much more photostable (Chan and Nie, 1998). Moreover, the exceptional amplification power of the DSN, the cumulative nature of the signal generation process, and the high fluorescence intensity of QDs permitted the detection of DVs down to $10^2$ viral RNA strands/μL. The excellent mismatch discrimination ability of the DSN will allow DVs to be detected with high confidence. The isothermal amplification scheme coupled to the simple assay protocol will make direct, rapid, and ultrasensitive detection of DVs in pristine clinical samples with little sample preparation possible.

## 2. Experimental section

### 2.1. Materials and apparatus

The DSN (EC 3.1.30.-, extracted from *Paralithodes camtschaticus*) was purchased from Evrogen (Moscow, Russia). Exonuclease I (Exo I) was purchased from New England Biolabs (Ipswich, MA, USA). Four types of carboxylic acid-coated CdSeS/ZnS alloyed QDs with $\lambda_{em}$ at 450, 520, 580, and 660 nm were purchased from Sigma-Aldrich (St. Louis, MO). Dual-labeled (terminal amine and biotin) DNA CPs of the following sequences: 5′-$A_9$ TGA TAT GTC TCT GAG TAT GTA TCC AAG TT $A_9$ (for DV-1), 5′-$A_9$ GGA AAT GTC CCT TAA TAT GTA GCC TAG CT $A_9$ (for DV-2), 5′-$A_9$ GCT CAC ATC TCT TAA AAT GTA GCC TAG CC $A_9$ (for DV-3), 5′-$A_9$ GTC TAT CTC CTC CAG GAT ATA TCC CAA TC $A_9$ (for DV-4), synthetic RNAs, and all other oligonucleotides of PCR purity were obtained from Integrated DNA Technologies (Coralville, IA, USA). Ethyl (dimethylaminopropyl) carbodiimide (EDC) was purchased from Pierce (Rockford, IL, USA). Streptavidin-coated magnetic beads were acquired from Life Technologies (Carlsbad, CA, USA). The hybridization/DSN incubation medium was made of pH 8.0 50 mM Tris buffer containing 20 mM $MgCl_2$ and 1.0 mM DTT (TMD buffer). All centrifuge tubes were autoclaved and all surfaces were treated with RNaseZap to eliminate any possible RNase contaminations. Nuclease-free ultrapure water was used in all solutions preparations. Fluorescence spectra were acquired on a Fluorolog®-3 spectrofluorometer (Jobin Yvon Inc., Edison, NJ, USA) using a microcuvette.

### 2.2. Preparation of the QD–CP tethered magnetic beads

The four types of CPs were first conjugated to their respective QDs through carbiimide coupling chemistry. Briefly, the carboxylic acid-coated QDs were suspended in 200 μL of pH 5.5 10 mM phosphate buffer. Then, the amine-terminated CPs were added into above solution with a final concentration of 1.0 μM. Subsequently, 100 μL of 0.020% freshly-prepared EDC solution was added and the reaction mixture was incubated for 24 h at room temperature with gentle shaking. After centrifugation, the supernatant was carefully removed. Purification of the QD–capped CPs (QD–CPs) form excess oligonucleotides was performed by three cycles of repetitive centrifugation and dispersion of the QD–CPs after conjugation. The purified QD–CPs were then tethered to the magnetic beads by incubating them with the streptavidin-coated magnetic beads in pH 8.0 10 mM Tris buffer containing 10 mM EDTA and 0.20 M NaCl for 30 min. Thereafter, the excess of CPs on the QDs was hydrolyzed into mononucleotides by a period of 60 min incubation with Exo I, whereas the CPs linked to the magnetic beads remained intact because of significant steric hindrance and terminal protection. It was found that $\sim 4.5 \times 10^5$ QD–CPs are attached to each magnetic bead, which is ~20% of the binding capacity of the magnetic beads (Invitrogen, 2011). After three thorough washes with ultrapure water, the QD–CP-tethered magnetic beads were kept in the dark at 4 °C in a refrigerator and ready for use. The QD–CPs tethered to the magnetic beads were stable for at least six months. However, the fluorescence intensity of the QDs was found to decrease over a much longer storage time due to the deterioration of the QDs.

### 2.3. DV detection and serotyping

Total RNA in DV was extracted using a viral RNA extraction kit from Qiagen (Valencia, CA, USA) according to the manufacturer′s recommendation. Briefly, 0.50 mL of DV sample was added to 5 mL of Qiazol solution. The mixture was vortexed and incubated for 15 min at room temperature. After adding 1.0 mL of chloroform the mixture was thoroughly mixed and centrifuged at $1.3–1.5 \times 10^4$ g for 10 min at 4 °C. The total RNA in the aqueous phase was further purified according the procedure recommended by the manufacturer. DV detection and serotyping were performed in microplates or microcentrifuge tubes. Each reaction mixture contains 1 × TMD buffer, 0.5 U/μL of RNase inhibitor, 500 nM QD–CPs, and 0.50 U the DSN. The total volume of the reaction mixture was $\leq 20$ μL. The obtained mixture was incubated at room temperature for 60 min to allow target RNA hybridization and the QD–CP cleavage. After removing the magnetic beads together with the unreacted QD–CPs, the fluorescence intensities of the cleaved QDs were used to quantify DVs and their emission profiles (emission wavelengths) were used to serotype DVs. In addition, a control was run in parallel for each assay. The control solution contained all components of the assay and a totally noncomplementary synthetic RNA. The fluorescence readings were always subtracted from that of the control.

## 3. Results and discussion

### 3.1. Assay strategy

The working principle of the assay is schematically described in Fig. 1. As shown in Fig. 1, the principal steps of the assay are: (a) preparation of the QD–CP-magnetic bead conjugates, (b) hybridization of DV RNA strands to the DNA CPs to form RNA–DNA heteroduplexes, (c) cleavage of the CPs in the heteroduplexes by the DSN and freeing the target RNA stands, (d) hybridization of the freed target RNA strands to the remaining QD–CPs on the magnetic beads – the establishment of an isothermal target cycling amplification process, and (e) magnetic separation of the magnetic beads along with unreacted QD–CPs. As a result, a large amount of the highly fluorescent QDs are released in solution, resulting in the appearance of a fluorescence signal. The target-recycling amplification and the cumulative nature of the DSN cleavage process eventually lead to significant signal enhancement when a sufficient amount of the DSN is used and a long enough hybridization/DSN incubation time is employed. DV serotyping is accomplished

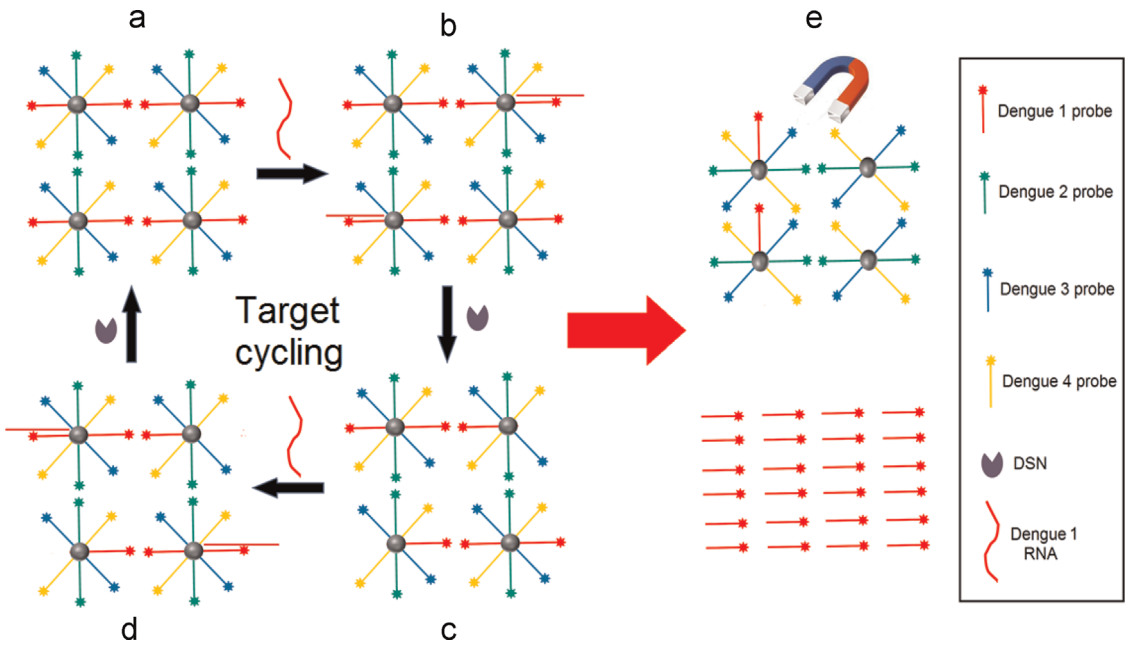


**Fig. 1.** Schematic representation of the working principle of the proposed DV assay.

by the characteristic emissions (colors) of the four types of the QDs.

### 3.2. Functionalization of the magnetic beads

Since the QDs serve as both signal generators and DV serotyping agents, they should have comparable size, shape, and fluorescence efficiency (quantum yields) but with distinctly different emission profiles. Obviously, the most popular size-tuned QDs are inappropriate to tag the CPs due to their significant difference in size and quantum yield. In contrast, the composition-tuned (alloyed) CdSeS/ZnS QDs are well-suited for our purpose. As illustrated in Fig. 2, the QDs displayed four distinct emissions, blue (for DV-1), green (for DV-2), yellow (for DV-3), and red (for DV-4,) with similar fluorescence efficiencies. More importantly, the four distinct colors persisted with a single excitation wavelength of 365 nm after they were conjugated to the magnetic beads, thus paving the way for both DV detection and serotyping. The fluorescence intensity reflects the copy number and the four colors represent the respective four serotypes of DVs. In addition, their uniformed size (~6 nm) is comparable to the size of the DSN (~4.7 nm), which is advantageous in the configuration of the assay since the DSN is be able to freely access the CPs without sacrificing the surface coverage. On the other hand, the magnetic beads serve as both the QD–CP carriers and the vehicles for the magnetic separation of the unreacted QD–CPs. Therefore, successful functionalization of the magnetic beads with the QD–CPs is a crucial step for realizing the proposed assay. To minimize steric hindrance, streptavidin-coated magnetic beads and the dual-labeled CPs with two $(A)_9$ terminal spacers were used to functionalize the magnetic beads. After the conjugation of biotin to streptavidin, unreacted and nonspecifically-adsorbed QD–CPs were cleaned up by three thorough washes of the functionalized magnetic beads in the washing buffer.

The accessibility the immobilized CPs for the hybridization with DV RNA was first evaluated by hybridizing the QD-CP-tethered magnetic beads with a fully complementary FAM-labeled synthetic target. As shown in Fig. 3, the supernatant of the QD–CP-

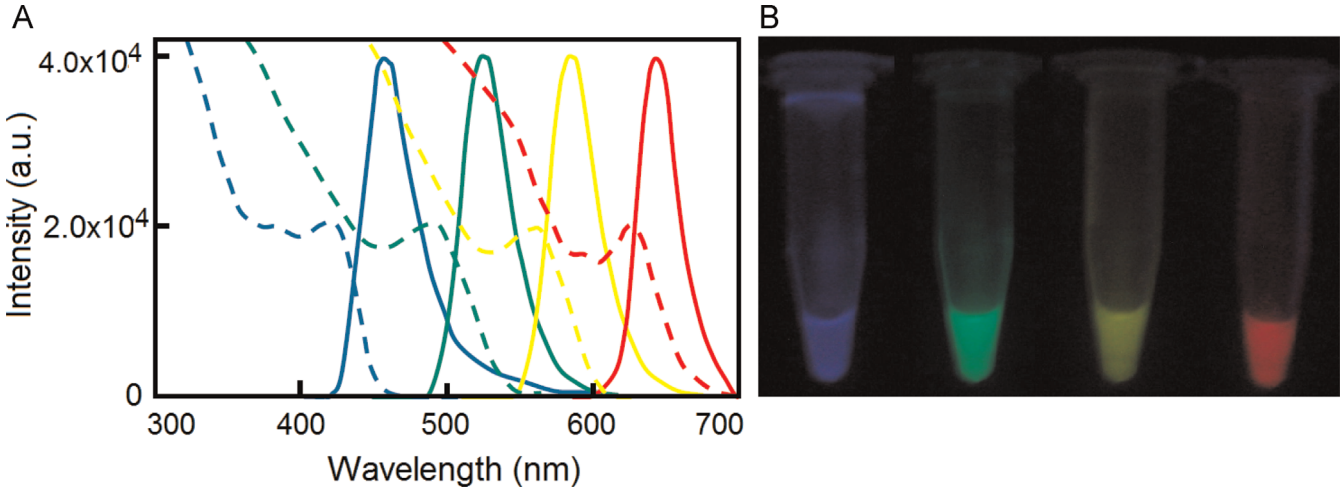


**Fig. 2.** (A) Excitation (dotted lines) and emission spectra (solid lines) of the CdSeS/ZnS alloyed QDs and (B) fluorescence emissions of the CdSeS/ZnS alloyed QDs conjugated to the magnetic beads excited at 365 nm. (For interpretation of the references to color in this figure the reader is referred to the web version of this article.)

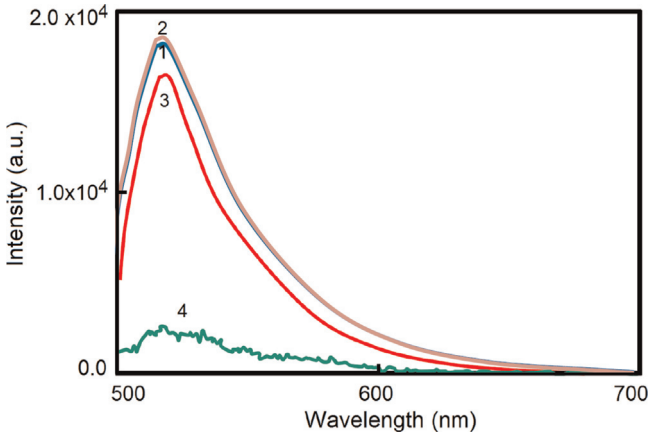


**Fig. 3.** Fluorescence responses of 0.20 μM FAM-tagged control (1) before and (2) after hybridization with the QD–CP-tethered magnetic beads; and 0.20 μM FAM-tagged target (3) before and (4) after hybridization with 500 nM QD–CP-tethered magnetic beads. 60 min hybridization in pH 8.0 50 mM Tirs buffer containing 0.10 M NaCl. For clarity, curve 4 was magnified 10 times.

tethered magnetic bead-treated control solution (containing 0.2 μM noncomplementary FAM-labeled RNA) exhibited a fluorescence intensity practically identical to that of the same solution before the treatment (Fig. 3 curves 1 and 2). The negligible change in florescence intensity before and after the treatment suggested that non-specific adsorption of the RNA sequences on the QD–CP-tethered magnetic beads is insignificant. This is probably due to strong repulsion between the anionic RNA strand and the high density of negative charges (arising from the CPs) on the magnetic bead's surface. On the other hand, the sample solution (0.2 μM the FAM-labeled fully complementary target) before the addition of the QD–CP-tethered magnetic beads was as high as $1.6 \times 10^4$ a.u. (Fig. 3 curve 3). The supernatant of the QD–CP-tethered magnetic bead-treated sample solution only gave a fluorescence intensity reading of 280 a.u., implying that the QD–CPs on the magnetic beads are fully functional and highly efficient in capturing their target sequences (Fig. 3 curve 4).

### 3.3. Feasibility study

As proof of concept, we first examined the feasibility of utilizing QDs and the DSN in sensitively detecting DV by observing the development of fluorescence signals when the DSN was added to the mixture of the QD–CP-tethered magnetic beads and 10 pM synthetic DV-2 and DV-4 RNAs. A non-complementary RNA of the same length was used as the control. Fig. 4 depicts typical time-dependent responses of the DV RNAs and the control. As

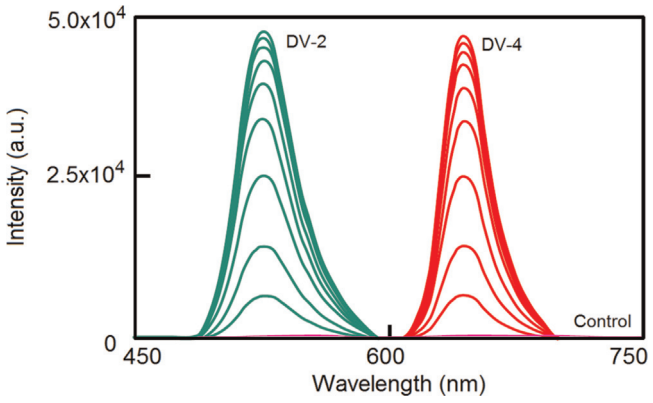


**Fig. 4.** Time-dependent responses (5-min intervals) of 10 pM DV-2, DV-4, and the control in TMD buffer containing 0.50 U the DSN and 500 nM QD–CPs at 50 °C.

seen in Fig. 4, a distinct difference between the DV RNAs and the control was obtained: only the DV RNAs that were complementary to the CPs tethered on the magnetic beads showed a progressive development of fluorescence, whereas negligible fluorescence was observed for the control throughout the entire period of incubation. These results suggested that the amount of the QDs is continuously cleaved off the magnetic meads during the hybridization/DSN incubation with the target RNAs, thus implying that the QD–CPs are capable of capturing the target DV RNAs and allowing free access by the DSN. Due to the relatively large size of the QD tags, steric hindrance is expected when the end of the hybridization region of the CPs is directly linked to the QDs. A spacer of appropriate length is needed to alleviate this problem. Experiments were therefore conducted to investigate the optimal length of the spacer. Normalized fluorescence responses of QD–CPs with poly (A) spacers were found to be 0.15, 0.45, 1.0, 1.04, and 1.02 for 3, 6, 9, 12, and 15 adenosines, respectively, thereby suggesting that a spacer with at least nine nucleotides between the QD and the DV capturing segment of the CP is necessary in order not to impose any steric hindrance to the DSN. Much longer spacers did not bring in any appreciable benefit. To keep the cost low, a nine-adenosine spacer was used in the construction of the QD–CPs. The above results also showed that only the DNA CPs in the DNA–RNA heteroduplexes are efficiently cleaved by the DSN. The target RNA strands are not degraded and readily rehybridize with the remaining QD–CPs on the magnetic beads, thereby establishing a cumulative target cycling amplification process.

Moreover, it has been shown that the DSN is practically inactive toward single-stranded DNA and RNA/RNA homoduplexes (Evrogen, 2012; Shagin et al., 2002). Indeed, being totally non-complementary to the CPs, no appreciable increases in fluorescence were observed for the control after identical treatments because the DSN is inactive toward the single-stranded CPs and the magnetic separation completely removes all magnetic beads along with the uncleaved QD–CPs from the solution. On the other hand, in the absence of the DSN, even though the target RNAs are perfectly complementary to the QD–CPs, after all treatments, the fluorescence spectrum was featureless (identical to that of the control), signifying that the QDs remain firmly attached to the magnetic beads and the magnetic separation completely removes all magnetic beads together with the QD–CPs from the solution. Also, the above results suggested that it is possible to realize ultrasensitive detection of DVs via DSN amplification.

### 3.4. Optimization

To develop an ultrasensitive assay for DV, the cumulative nature of the DSN cleaving process must be thoroughly investigated since the performance of the assay is primarily dependent on the quantity of the cleaved QDs, which is determined by the concentration of the target, hybridization time, and the DSN cleavage efficiency. Unfortunately, the coordinated hybridization and DSN cleavage suggests that the analytical signal (fluorescence intensity) of the assay is codependent on both the target and the DSN concentrations. Therefore, the optimization of the experimental conditions, particularly the DSN concentration, and the construction of the calibration curve of the assay is somehow subjective. Nonetheless, our interest was to develop a DV assay that is capable of detecting the lowest possible levels of DV ( $\leq$ femtomolars). In principle, provided that there is a sufficient amount of the QD–CPs on the magnetic beads, the highest possible concentration of the DSN should be employed in all experiments to safeguard the highest efficiency of the CP cleavage process and to have a sole dependence of the amount of the cleaved QDs on the target RNA concentration. Under this circumstance, the cleavage of the QDs from the magnetic beads is solely associated with the

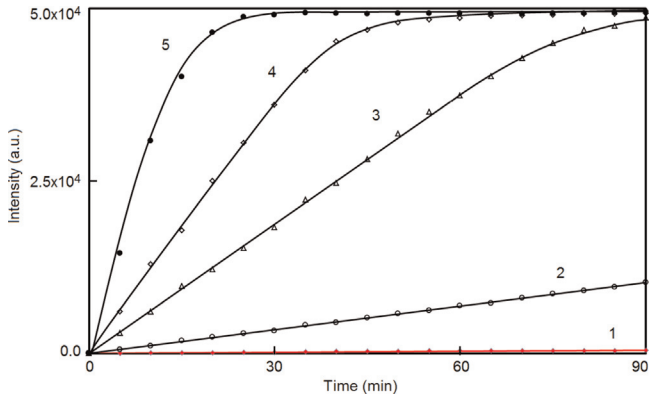


**Fig. 5.** The dependence of fluoroscence intensity at 520 nm on hybridization/DSN incubation time. (1) Control, (2) 10 fM (3) 250 fM, (4) 500 fM, and (5) 2.0 pM DV-2 RNA in TMD buffer containing 0.50 U the DSN and 500 nM QD–CPs at 50 °C.

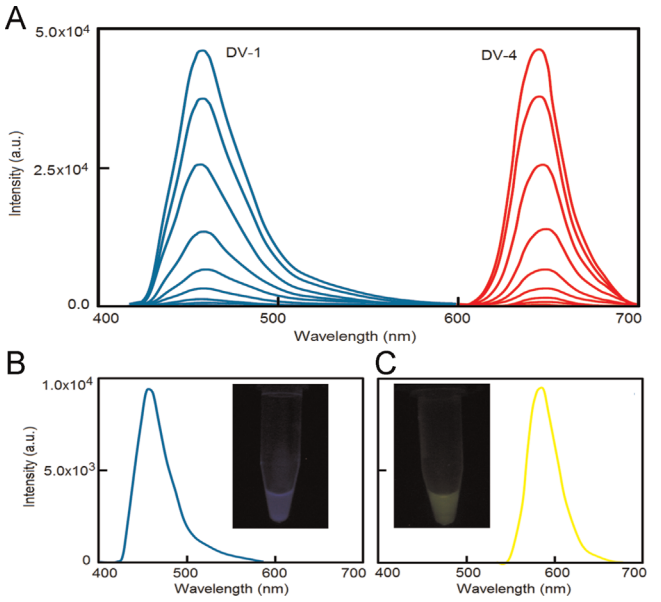


**Fig. 6.** (A) Fluorescence responses of DV-1 and DV-4 in calibration study (From bottom to top: 1, 5, 10, 25, 50, 100, 200, 300, 400 fM), (B) fluorescence response of DV-1 specific QD–CP-tethered magnetic beads to a mixture of total RNAs from all four serotypes and (C) fluorescence response of the four types of QD–CP-tethered magnetic beads to total RNA extracted from DV-3.

hybridization efficiency. The high concentration of the DSN warrants that the CP cleavage rate is not dependent on the DSN but solely on the number of hybridized DNA–RNA heteroduplexes, which infers that the sensitivity of the assay would scale up with the hybridization/incubation time. Taking into consideration of the cost of the DSN, it was found that 0.50 U DSN is enough for the detection of DV down to femtomolar levels.

As depicted in Fig. 5, in the presence of 0.50 U DSN and 500 nM QD–CPs, the fluorescence intensity versus hybridization/DSN incubation time showed a nonlinear pattern. At low target concentration of 10 fM, the fluorescence intensity increased linearly throughout, suggesting that there is little loss of the DSN activity during the hybridization/DSN incubation. However, as seen in Fig. 5, for relatively high concentrations of the DV RNA, for example 500 fM and 2.0 pM, the fluorescence intensity gradually approached a steady-state after 60 and 30 min of hybridization/DSN incubation, respectively. In addition, the fluorescence intensity of the control remained relatively low throughout the entire period of 90 min incubation, suggesting that there are no noticeable detachments of the QDs from the magnetic beads. Consequently, a sufficiently long period of hybridization/DSN incubation is expected to produce a high sensitivity for the detection of extremely low levels of DVs. To have a high sensitivity while keeping a reasonably turnaround time, it was found that femtomolars of DV can be unambiguously detected after a period of 60 min hybridization/DSN incubation.

### 3.5. Calibration study

With this characteristic fluorescence generation process associated with the hybridization of the target DV RNA and subsequent cleavage of the QDs by the DSN, further investigations were conducted to establish the correlation between the fluorescence intensity and the target DV RNA concentration. For successfully adapting the DSN-mediated target cycling amplification scheme in the development of an ultrasensitive DV assay, the analytical signal must be exclusively correlated to the concentration of the DV, desirably a straightforward linear relationship between the fluorescence intensity and the target RNA concentration. In the presence of 0.50 U DSN and 500 nM QD–CPs, a period of 60 min hybridization/DSN incubation produced a linear correlation between the fluorescence intensity and the target RNA concentration between 1.0 and 300 fM ($y=126x+185$, $R^2=0.98$) (Fig. 6A) with a detection limit of 0.50 fM (300 RNA strands/μL) at a signal-to-noise ratio of 3.0 ($3\sigma$, three times of the standard derivation of the control), representing four orders of magnitude improvement over previous QD-based nucleic acid assays (Gao et al., 2011; Wu and Yan, 2013; Gerion et al., 2003). Nonetheless, the cumulative nature of the signal generation process offered a versatile means to substantially enhance the sensitivity of the assay. For example, a period of 12 h hybridization/DSN incubation produced a detection limit as low as 50 aM, corresponding to 30 target RNA strands/μL. On the other hand, as a practically homogeneous assay, much improved reproducibility was expected (Yang et al., 2014; Deng et al., 2013, 2014; Gao et al., 2013; Shen et al., 2013, 2012). For instance, the standard derivations of 10 duplicated tests at 2.0 and 200 fM were found to be 9% and 7%, respectively.

### 3.6. Selectivity

DV infection shares similar symptoms with other closely related mosquito-borne flaviviruses, such as Yellow Fever (YF), Japanese Encephalitis (JE), and Chikungunya virus (CHIK). A DV assay must be able to unambiguously distinguish DV from other mosquito-borne flaviviruses. The specificity of the assay was therefore evaluated against other flaviviruses. Total RNA samples extracted from these virus stocks of YF, JE and CHK were tested by the proposed assay. The results indicated that none of the RNA samples tested showed positive responses ($<3\sigma$ of the noise of the control), suggesting that the proposed assay is highly specific to DV. Moreover, the capability in selectively detecting a specific DV (serotyping) is essential in epidemiological surveillance. Further to efficiently cleaving the DNA strands in RNA–DNA heteroduplexes, it has been reported that the DSN selectively acts on the DNA strands in fully complementary RNA–DNA heteroduplexes while remains inactive towards mismatched ones.

To evaluate the selectivity for serotyping DV, the proposed assay was further tested for its ability to serotype DV in total RNA extracted from the supernatant of DV infected cell culture. First, DV-1 specific QD–CP-tethered magnetic beads were placed in a mixture of total RNAs extracted from all four types of DVs. As shown in Fig. 6B, the DV serotype-specific CPs positively detected their corresponding DV serotype as signified by a distinctive appearance of fluorescence signal at designated wavelength. Then, all four types of QD–CP-tethered magnetic beads in equal amounts were incubated with a total RNA sample extracted from DV-3

culture. The appearance of the fluorescence emission at 520 nm and the yellow color of the fluorescence emission unambiguously confirmed that among the four types of the QD–CP-tethered magnetic beads only the DV-3 specific ones reacted with the DV-3 RNA without any notable cross-reaction (Fig. 6C). These results clearly demonstrated that the proposed assay is capable of detecting DV in a serotype-specific manner with high sensitivity. Unlike the two-step NASBA amplification and hybridization and ECL detection procedure (Wu et al., 2001), the amplification, detection, and serotyping of DVs were accomplished in one step in a single tube within a shorter period of time. In principle, DV detection could be achieved with a very simple device, for example a battery-powered UV lamp since the QDs can be excited at any wavelength beyond the shortest absorption wavelength of the QDs.

## 4. Conclusion

In this report we demonstrated that the QD–CPs in conjunction with the DSN cleavage (amplification) can be utilized to devise a simple and ultrasensitive assay for the detection and serotyping of DVs. The combination of the DSN and QD–CPs led the unique DSN-mediated target cycling amplification and ultrasensitive fluorescence detection. The adoption of the magnetic beads as the QD–CP carriers facilitated a highly reproducible homogeneous hybridization with much improved hybridization efficiency and provided a convenient means of easy separation of the unreacted QS–CPs. The ultrahigh sensitivity circumvented the engagement of PCR and the freedom from target tagging greatly improved the suitability in direct detecting and serotyping of DV with minimal or no sample pre-treatments. The demonstrated capability of the proposed assay in highly selective detection and serotyping of DV clearly suggested that it is an attractive candidate for the development of a fast, simple, and robust assay for ultrasensitive detection and serotyping of DVs at point-of-care.

## Acknowledgments

The authors thank Ministry of Education for the financial support.

## References

Chan, W.C.W., Nie, S.M., 1998. Science 281, 2016–2018.
Deng, H.M., Ren, Y.Q., Shen, W., Gao, Z.Q., 2013. Chem. Commun. 49, 9401–9403.
Deng, H.M., Shen, W., Ren, Y.Q., Gao, Z.Q., 2014. Biosens. Bioelectron 54, 650–655.
Endy, T.P., Chunsuttiwat, S., Nisalak, A., Libraty, D.H., Green, S., Rothman, A.L., Vaughn, D.W., Ennis, F.A., 2002. Am. J. Epidemiol. 156, 40–51.
Gao, Y.L., Stanford, W.L., Chan, W.C.W., 2011. Small 7, 137–146.
Gao, Z.Q., Deng, H.M., Shen, W., Ren., Y.Q., 2013. Anal. Chem. 85, 1624–1630.
Gerion, D., Chen, F.Q., Kannan, B., Fu, A.H., Parak, W.J., Chen, D.J., Majumdar, A., Alivisatos, A.P., 2003. Anal. Chem. 75, 4766–4772.
Gijavanekar, C., Anez-Lingerfelt, M., Feng, C., Putontim, C., Fox, G.E., Sabo, A., Fofanov, Y., Willson, R.C., 2011. FEBS J. 278, 1676–1687.
Gubler, D.J., 1998. Clin. Microbiol. Rev. 11, 480–496.
Guzman, M.G., Halstead, S.B., Artsob, H., Buch, P., Farrar, J., Gubler, D.J., Hunsperger, E., Kroeger, A., Margolis, H.S., Martínez, E., Nathan, M.B., Pelegrino, J.L., Simmons, C., Yoksan, S., Peeling, R.W., 2010. Nat. Rev. Microbiol. 8, S7–S16.
Pritchard, C.C., Cheng, H.H., Tewari, M., 2012. Nat. Rev. Genet. 13, 358–369.
Ranjit, S., Kissoon, N., 2011. Pediatr. Crit. Care Med. 12, 90–100.
Scott, H.B., 2007. Lancet 370, 1644–1652.
Shagin, D.A., Rebrikov., D.V., Kozhemyako, V.B., Altshuler, I.M., Shcheglov, A.S., Zhulidov, P.A., Bogdanova, E.A., Staroverov, D.B., Rasskazov, V.A., Lukyanov, S., 2002. Genome Res. 12, 1935–1942.
Shen, W., Lim, C.L., Gao, Z.Q., 2013. Chem. Commun. 49, 8114–8116.
Shen, W., Deng, H.M., Gao, Z.Q., 2012. J. Am. Chem. Soc. 134, 14678–14681.
Whitehead, S.S., Blaney, J.E., Durbin, A.P., Murphy, B.R., 2007. Nat. Rev. Microbiol. 5, 518–528.
Whitehorn, J., Farrar, J., 2010. Br. Med. Bull. 95, 161–173.
Wiwanitkit, V., 2010. Expert. Rev. Anti infect. Ther. 8, 841–845.
World Health Organization, 1997. Dengue haemorrhagic fever: diagnosis, treatment, prevention and control, second ed. Geneva, Switzerland.
Wu, S.-J.L., Lee, E.M., Putvatana, R., Shurtliff, R.N., Porter, K.R., Suharyono, W., Watts, D.M., King, C.-C., Murphy, G.S., hayes, C.G., Romano, A.J., 2001. J. Clin. Microbiol. 39, 2794–2798.
Wu, P., Yan, X.P., 2013. Chem. Soc. Rev. 42, 5489–5521.
Yang, X.J., Yu, Y.B., Gao, Z.Q., 2014. ACS Nano 8, 4902–4907.
World Health Organization, 2014. ⟨http://www.who.int/topics/dengue/en/⟩.
Invitrogen, 2011. http://tools.lifetechnologies.com/content/sfs/manuals/dynabeads_m280SAv_man.pdf.
Evrogen, 2012. ⟨http://www.evrogen.com/products/DSN/DSN.shtml⟩.